

Extended local Rytov Fourier migration method

Lian-Jie Huang*, Michael Fehler, and Peter Roberts, Los Alamos National Laboratory
Charles Burch, Conoco, Inc.

Summary

There is a vital need for an efficient and accurate migration method capable of imaging large 3D complex structures which are difficult for a ray-tracing based Kirchhoff migration method to image. We develop a novel depth migration method termed the extended local Rytov Fourier migration method. It is based on the scalar wave equation and a local application of the Rytov approximation within each extrapolation interval. The method is efficient due to the use of a Fast Fourier Transform algorithm. While it is similar in implementation to the split-step Fourier migration approach, it is more accurate and can handle amplitudes of wavefields more reliably than the split-step Fourier method. The stability of the method is controlled more easily than that of the extended local Born Fourier method that we previously investigated. Migration examples for a 2D slice of the SEG/EAGE model and the Marmousi model are given to demonstrate the method.

Introduction

Imaging 3D complex structures has become a great challenge in recent years. For imaging complex structures, there is a need for a reasonably accurate method that is faster than the finite-difference wave-equation based migration methods. The phase-shift plus interpolation method (Gazdag and Sguazzero, 1984) and the split-step Fourier method (Stoffa et al., 1990) are wave-equation based methods and can handle complex structures better than the commonly used ray-tracing based Kirchhoff migration method. The physical basis of the phase-shift plus interpolation and the split-step Fourier methods are the same (Popovici, 1996; Huang et al., 1997). Another Fourier transform based migration method termed the extended local Born Fourier method was developed recently (Huang and Fehler, 1997; Huang et al., 1997). It can handle a wider angle than the split-step Fourier method for a given level of imaging error. It utilizes the Born approximation within each extrapolation interval.

We develop an alternative Fourier transform based method using the Rytov approximation within each extrapolation interval. The method is termed the extended local Rytov Fourier migration method. It takes into account the multiple forward scattering due to lateral slowness perturbations. Its stability is controlled much more easily than that of the extended local Born Fourier method. Under the small angle approximation, the extended local Rytov Fourier method converges to the split-step Fourier method. We first give the formulation of the extended local Rytov Fourier method, then use the method to migrate exploding reflector data for a 2D slice

of the SEG/EAGE salt model (Aminzadeh et al., 1996) and the shot-gather dataset for the Marmousi model to demonstrate the applicability of the method. It has also been used to migrate a 2D field shot-gather dataset provided by Conoco (Fehler, et al., 1998)

Method

The constant density scalar wave equation in the frequency domain is given by

$$\left[\frac{\partial^2}{\partial x^2} + \frac{\partial^2}{\partial y^2} + \frac{\partial^2}{\partial z^2} + \frac{\omega^2}{v^2(\mathbf{x}_T, z)} \right] p(\mathbf{x}_T, z; \omega) = 0, \quad (1)$$

where $\mathbf{x}_T \equiv (x, y)$, $p(\mathbf{x}_T, z; \omega)$ is the pressure in the frequency domain, $v(\mathbf{x}_T, z)$ is the velocity of the medium, and ω is the circular frequency. Making use of the Rytov approximation within each extrapolation interval, we obtain the wavefield extrapolation equation from z_i to z_{i+1} given by

$$p(\mathbf{x}_T, z_{i+1}; \omega) = p_0(\mathbf{x}_T, z_{i+1}; \omega) e^{i\omega \left[\int_{z_i}^{z_{i+1}} \Delta s(\mathbf{x}_T, z) dz \right]} \chi(\mathbf{x}_T, z_{i+1}; \omega), \quad (2)$$

where $p_0(\mathbf{x}_T, z_{i+1}; \omega)$ is obtained by

$$p_0(\mathbf{x}_T, z_{i+1}; \omega) = \mathcal{F}_{\mathbf{k}_T}^{-1} \left\{ e^{ik_{0z} \Delta z} \mathcal{F}_{\mathbf{x}_T} \{ p(\mathbf{x}_T, z_i; \omega) \} \right\}, \quad (3)$$

and $\chi(\mathbf{x}_T, z_{i+1}; \omega)$ is defined by

$$\chi(\mathbf{x}_T, z_{i+1}; \omega) \equiv \frac{p_1(\mathbf{x}_T, z_{i+1}; \omega)}{p_0(\mathbf{x}_T, z_{i+1}; \omega)}, \quad (4)$$

with

$$p_1(\mathbf{x}_T, z_{i+1}; \omega) \equiv \mathcal{F}_{\mathbf{k}_T}^{-1} \left\{ \sigma(z_i) e^{ik_{0z} \Delta z} \mathcal{F}_{\mathbf{x}_T} \{ p(\mathbf{x}_T, z_i; \omega) \} \right\}. \quad (5)$$

In the above equations, $\Delta z = z_{i+1} - z_i$, $\mathbf{k}_T \equiv (k_x, k_y)$, \mathcal{F} and \mathcal{F}^{-1} represent respectively forward and inverse Fourier transforms, and $\Delta s(\mathbf{x}_T, z)$ is the slowness perturbation given by

$$\Delta s(\mathbf{x}_T, z) = s(\mathbf{x}_T, z) - s_0(z), \quad (6)$$

where s and s_0 are the slownesses of the real medium and the reference medium, respectively. The vertical component of wavenumber is

$$k_{0z} = \sqrt{k_0^2 - \mathbf{k}_T^2}, \quad (7)$$

Extended local Rytov Fourier method

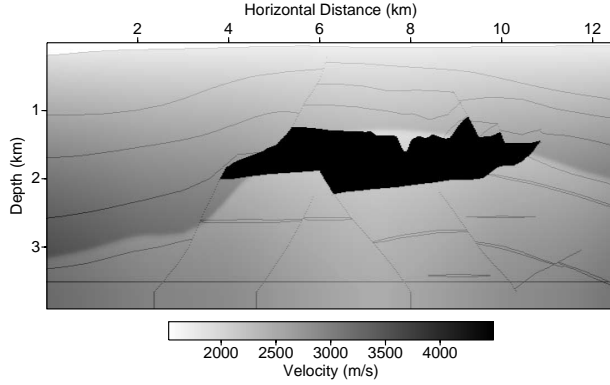


Fig. 1: A 2D slice of the SEG/EAGE 3D salt model. The dark black region is a salt body.

with $k_0 = \omega s_0$. The term $\sigma(z_i)$ is given by (see Huang et al., 1997)

$$\sigma(z_i) = 1 + 0.5 \left(\frac{k_T}{k_0} \right)^2 + 0.375 \left(\frac{k_T}{k_0} \right)^4 + 0.3125 \left(\frac{k_T}{k_0} \right)^6 + 0.2734375 \left(\frac{k_T}{k_0} \right)^8. \quad (8)$$

The denominator of equation (4) may be equal to or approach zero, and consequently equation (2) would diverge. To circumvent this numerical problem, we approximate χ as

$$\chi(\mathbf{x}_T, z_{i+1}; \omega) \approx \frac{p_1(\mathbf{x}_T, z_{i+1}; \omega) p_0^*(\mathbf{x}_T, z_{i+1}; \omega) + \delta}{p_0(\mathbf{x}_T, z_{i+1}; \omega) p_0^*(\mathbf{x}_T, z_{i+1}; \omega) + \delta}, \quad (9)$$

where “*” represents the complex conjugate and δ is a small real number that can be chosen as

$$\delta = \zeta [\max\{p_0(\mathbf{x}_T, z_{i+1}; \omega) p_0^*(\mathbf{x}_T, z_{i+1}; \omega)\}], \quad (10)$$

with a small real number of ζ . Equation (2) is termed the *extended local Rytov Fourier propagator*.

When the propagation angle relative to the main propagation direction (i.e. the positive direction of z -axis) is small, we have

$$\frac{k_0}{k_{0z}} \approx 1.$$

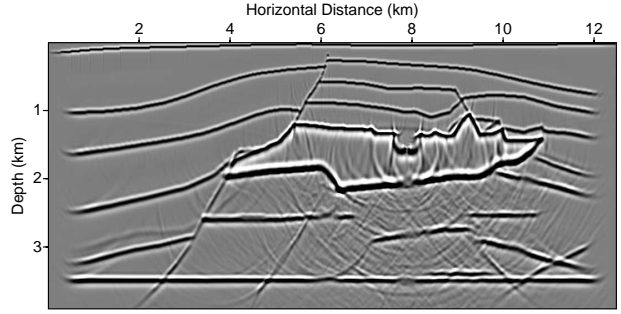
Making use of this approximation, equation (4) becomes

$$\chi(\mathbf{x}_T, z_{i+1}; \omega) \approx 1. \quad (11)$$

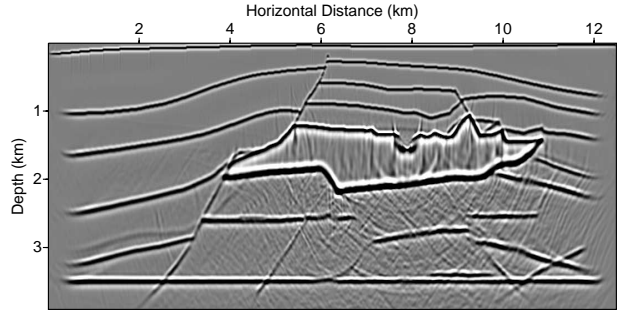
Then substituting equation (11) into equation (2) yields

$$p(\mathbf{x}_T, z_{i+1}; \omega) \approx p_0(\mathbf{x}_T, z_{i+1}; \omega) e^{i\omega \left[\int_{z_i}^{z_{i+1}} \Delta s(\mathbf{x}_T, z) dz \right]}. \quad (12)$$

Equation (12) is the split-step Fourier propagator (cf Stoffa et al., 1990; Huang and Wu, 1996; Huang and Fehler, 1998). Therefore, the split-step Fourier method can be considered as a small angle approximation of the extended local Rytov Fourier method.



(a) Split-step Fourier migration



(b) Extended local Rytov Fourier migration

Fig. 2: Migration images for a 2D slice of the SEG/EAGE model. The exploding reflector dataset used was generated by a finite-difference method.

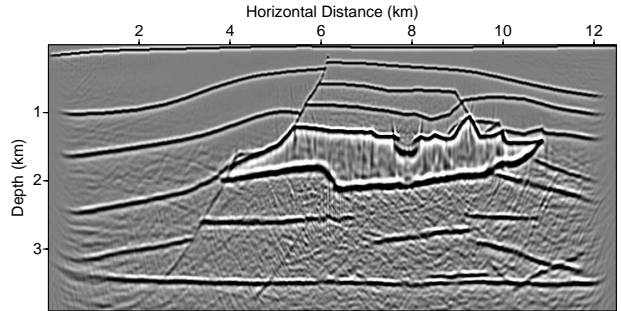


Fig. 3: Migration image for the 2D slice of the SEG/EAGE salt model obtained using the extended local Rytov Fourier method with $\delta = 0$ in the numerator of equation (9) but $\delta \neq 0$ in the denominator.

Migration of an exploding reflector dataset

We used a 2D slice of the SEG/EAGE salt model defined on a grid 1024×320 with a grid spacing of 12.192 m (see Figure 1) to test the capability of the extended local Rytov Fourier method to migrate a zero-offset dataset for a complex medium. The black region in Figure 1 represents a salt body. There are strong lateral velocity variations around this salt body. The exploding reflector dataset was generated using a finite-difference scheme with a 4th-order accuracy in space and a 2nd-order accu-

Extended local Rytov Fourier method

racy in time. Sources with a Ricker's time history were introduced along velocity interfaces. The central frequency of the Ricker's time history is 20 Hz. The frequency range used for migration is from 5 to 60 Hz with 226 frequency components. The average slowness within each extrapolation interval was used as a reference slowness. The value of ζ in equation (10) was chosen to be 0.05. Migrations were made using the split-step Fourier method and the extended local Rytov Fourier method and the images are respectively displayed in Figure 2(a) and (b). Images in Figure 2 show that the extended local Rytov Fourier method gives better images of the upper and lower salt interfaces and subsalt interfaces than the split-step Fourier method.

If we choose $\delta = 0$ in the numerator of equation (9) but $\delta \neq 0$ in the denominator, which follows the same approach used in deconvolution to eliminate a singularity, the corresponding extended local Rytov Fourier migration image is shown in Figure 3. The image in Figure 3 is not as good as that in Figure 2(b), which demonstrates the need of introducing a small number in the numerator of equation (9).

On an UltraSPARC computer with a CPU's clock rate of approximately 296 MHz, the extended local Rytov Fourier migration took approximately 4 minutes of CPU time while the split-step Fourier migration took approximately 3 minutes to migrate the 2D SEG/EAGE dataset.

Migration of the Marmousi dataset

The synthetic shot-gather dataset for the Marmousi model was used to test the capability of the extended local Rytov Fourier method to migrate a prestack dataset from a complex medium. The dataset was recently migrated using the split-step Fourier method (Roberts et al., 1997). A portion of the Marmousi velocity model is shown in Figure 4. The model was discretized with a horizontal grid spacing of 25 m and a vertical grid spacing of 4 m. The main imaging target is the anticlinal structure around the target region shown in the figure. The shot-gather dataset consists of 240 shots with 96 traces per shot. The time sample interval is 4 ms. The shot and receiver spacings are both 25 m. The first shot was located at $x = 3000$ m. Receivers were on the left hand side of each shot with a minimum offset of 200 m. The frequency range used during migrations is from 5 to 60 Hz with 226 frequency components. Migration images obtained using the split-step Fourier method and the extended local Rytov Fourier method are displayed in Figure 5. Comparing the region of the images within the ellipses in Figure 5(a) and (b), we see that the image in Figure 5(b) has a sharper definition than the one in Figure 5(a).

Figure 6 is a blow-up model near the target region of the Marmousi model. Figure 7 shows the images of the target region obtained using the different methods. The reflectors obtained using the extended local Rytov Fourier method have better continuity than those obtained with the split-step Fourier method.

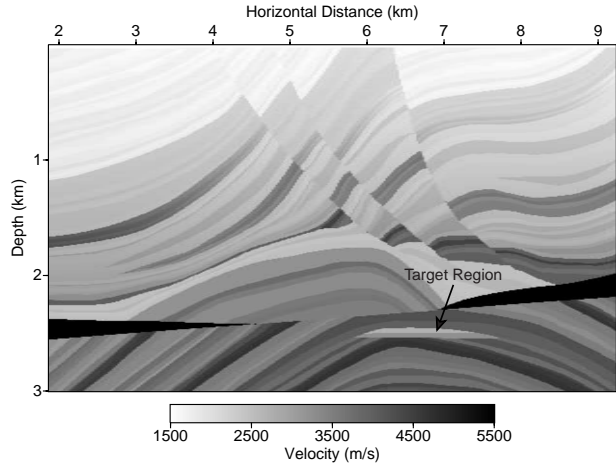


Fig. 4: Marmousi model.

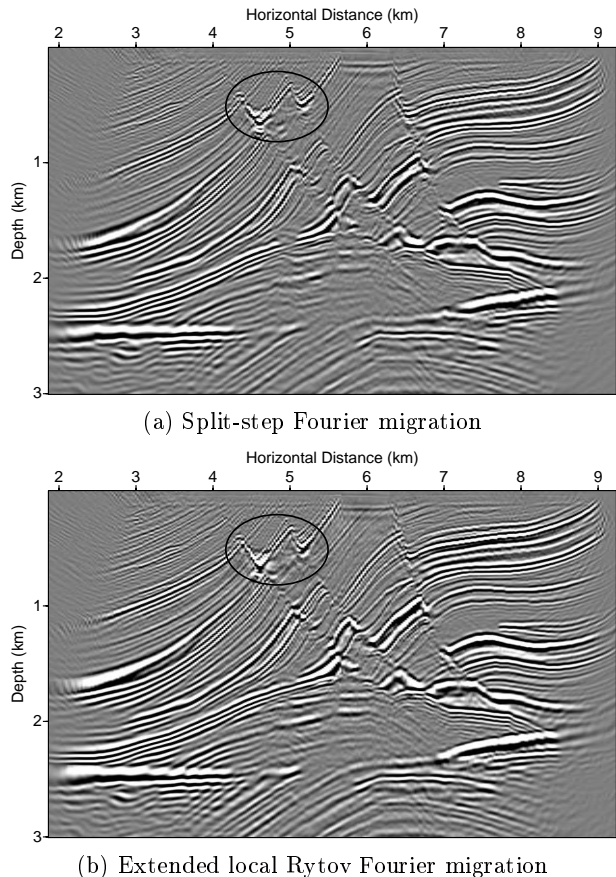


Fig. 5: Migration images for the Marmousi shot-gather dataset.

Extended local Rytov Fourier method

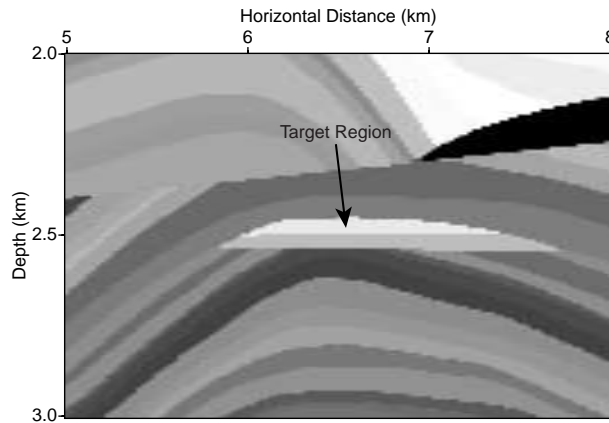


Fig. 6: Blow-up region around the target region in the Mar-mousi model

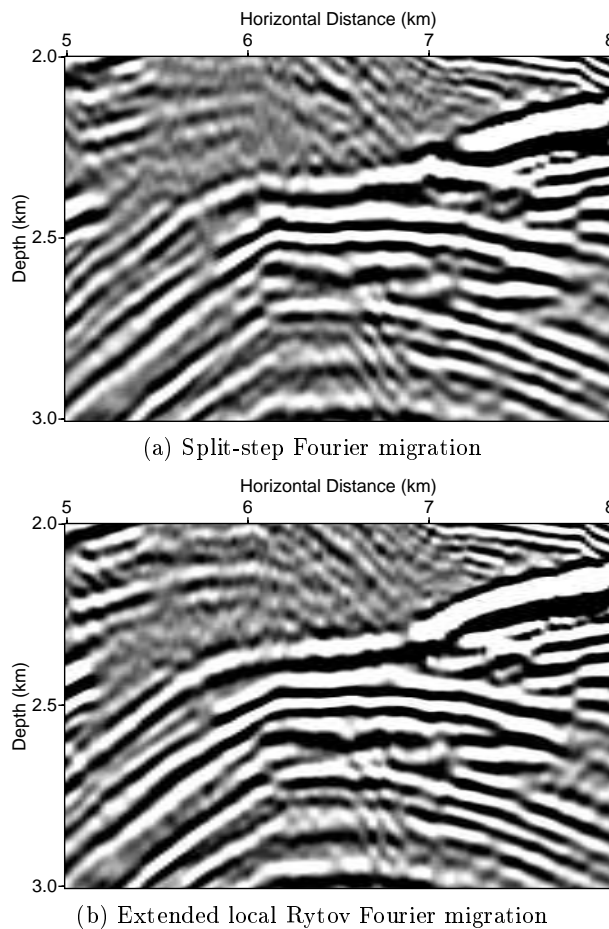


Fig. 7: Blow-up images around the target region.

Conclusions

We have developed an efficient wave-equation based migration method termed the extended local Rytov Fourier method. The method utilizes the Rytov approximation within each extrapolation interval. It can be used for imaging complex structures that are difficult for the commonly used ray-tracing based Kirchhoff migration method to image correctly. We have theoretically and numerically demonstrated that the extended local Rytov Fourier method can provide better images than the split-step Fourier method, especially for regions where structures are complex and wavefield amplitudes are important for imaging.

Acknowledgements

This work was funded by the Department of Energy Office of Basic Energy Sciences through contract W-7405-ENG-36 to the Los Alamos National Laboratory.

References

- Aminzadeh, F., Burkhard, N., Long, J., Kunz, T., and Duclos, P., 1996, Three dimensional SEG/EAGE models — an update: *The Leading Edge*, **15**, 131–134.
- Fehler, M., Huang, L.-J., Alde, D., Hildebrand, S., and Burch, C., 1998, Comparison of images obtained from a 2D Gulf of Mexico subsalt dataset using different migration approaches: submitted to the 68th Ann. Internat. Mtg., Soc. Expl. Geophys.
- Gazdag, J. and Sguazzero, P., 1984, Migration of seismic data by phase-shift plus interpolation: *Geophysics*, **49**, 124–131.
- Huang, L.-J. and Fehler, M., 1997, Extended pseudo-screen migration with multiple reference velocities: 67th Ann. Internat. Mtg., Soc. Expl. Geophys., Expanded Abstracts, 1742–1745.
- Huang, L.-J., Fehler, M., and Wu, R.-S., 1997, Extended local Born Fourier migration method: submitted to *Geophysics*.
- Huang, L.-J. and Fehler, M., 1998, Accuracy analysis of the split-step Fourier propagator: implications for seismic modeling and migration: *Bull. Seis. Soc. Am.*, **88**, 18–29.
- Huang, L.-J. and Wu, R.-S., 1996, Prestack depth migration with acoustic screen propagators: 66th Ann. Internat. Mtg., Soc. Expl. Geophys., Expanded Abstracts, 415–418.
- Popovici, A. M., 1996, Prestack migration by split-step DSR: *Geophysics*, **61**, 1412–1416.
- Roberts, P., Huang, L.-J., Burch, C., Fehler, M. C., and Hildebrand, S., 1997, Prestack depth migration for complex 2-D structure using phase-screen propagators: 67th Ann. Internat. Mtg., Soc. Expl. Geophys., Expanded Abstracts, 1282–1285.
- Stoffa, P. L., Fokkema, J. T., de Luna Freire, R. M., and Kessinger, W. P., 1990, Split-step Fourier migration: *Geophysics*, **55**, 410–421.